Journal of Interfaces, Thin films, and Low dimensional systems 5 (1) Summer and Autumn (2021) 455-465

The time delay between signals of tokamak magnetic coils and its effect on the measurement of plasma displacement

Scientific research paper

Ali Asghar Nasimi[1], Shervin Saadat[1*], Behzad Mansouri[1,2]

[1]*Department of Physics, Ahvaz Branch, Islamic Azad University, Ahvaz, Iran*

[2]*Department of Statistics, Shahid Chamran University of Ahvaz, Ahvaz, Iran*

ARTICLE INFO

Article history:
Received 30 January 2022
Revised 8 May 2022
Accepted 9 June 2022
Available online 8 July 2022

Keywords
Time series
Time delay
Phase shift
Plasma
Tokamak

ABSTRACT

The time delay between magnetic coil signals in a tokamak is believed to lead to inaccuracy in the measurement of the plasma physical parameters in the tokamak. In this research, we calculated the time delay between the signals of magnetic coils used in IR-T1 tokamak and investigated its effect on the measurement of the plasma horizontal displacement. The time delay between the signals of the magnetic coils was calculated utilizing time series analysis, and the horizontal displacement of the plasma was measured using the multipole moments method. The experimental results showed that by eliminating the time delay from the coil signals, the measurement of plasma horizontal displacement in IR-T1 tokamak was optimized.

1 Introduction

The position of plasma in tokamak was determined considering certain factors, such as plasma density, current density, soft x-ray, plasma pressure, and the tangential and normal components of the magnetic field that were induced by the plasma current. Measuring magnetic fields and also radiations caused by plasma current would give information regarding the plasma position in the tokamak. Plasma displacement measurement methods could be classified in to two general categories as magnetic and non-magnetic methods. In the non-magnetic method, certain diagnostics tools, such as Bolometer, Soft x-ray, and Longmuir Probes could be used [1]. In the magnetic method, plasma displacement could be measured with magnetic coils at several points (Mirnov method) [2] or along a closed contour (the multipole-moment method) around the plasma column [3, 4].

Spectral analysis of a time series (periodogram) and two-time series (coherence spectra) has proven to be a powerful technique for analyzing nonstationary plasma fluctuation data. Many of these analyses are based on Fourier techniques in which fluctuations can be expressed as a superposition of sinusoidal functions [5].

Tokamaks are electromagnetic systems composed of components, such as transformers, power supplies,

*Corresponding author.
Email address: Shervinsa27@Gmail.com
DOI: 10.22051/jitl.2022.39359.1066

windings, eddy currents, and toroidal and poloidal magnetic fields induced by plasma current. Therefore, the time delay between the signals of tokamak magnetic coils is inevitable. Thus, the existence of this time delay between the coil data could impair the accuracy of the measured plasma parameters in the tokamak. Measuring and remediation of time-delay effects in tokamaks have always been of interest to researchers [6, 7].

Several studies have been conducted to measure the plasma position using magnetic coil signals in IR-T1 tokamak [8, 9]. In this paper, we have calculated the time delay between the magnetic coil signals of IR-T1 tokamak and investigated its effect on the measurement of the plasma horizontal displacement. Time-series analysis have been used for measuring the time delay between coil signals [10].

This paper is arranged as follows: In Section 2, the details of the time series analysis theory are presented. In Section 3, the experimental setup for detecting plasma components is described. In Section 4, the time delay between the signals of the IR-T1 tokamak coils is calculated using the cross-spectral analysis. Section 5 discusses the details of the multipole moments method to measure the plasma horizontal displacement. In Section 6, the effect of time delay between the magnetic coils signals on the measurement of plasma horizontal displacement in IR-T1 tokamak is investigated and the results are reported. The conclusions are provided in Section 7.

2 Time series analysis

2.1 Periodogram

A time series is known as a set of statistical data collected at regular time intervals. Time series analysis comprises methods for analyzing time-series data in order to extract meaningful statistics and other characteristics of the data. One of these methods is cross-spectral analysis. The cross-spectral analysis is an extension of single spectrum analysis to the simultaneous analysis of two time series and it aims to unfold the correlations between two time series at different frequencies. The spectrum, as the main feature of a given time series in the Fourier domain, is estimated with a periodogram, which is a powerful technique for studying the hidden periodicities in time series [11, 10].

Suppose that $\{z_t\}_{t=1}^{n}$ is a time series and z_t is a random variable. Fourier representation of z_t is defined as

$$z_t = \sum_{k=0}^{[n/2]} (a_k \cos\omega_k t + b_k \sin\omega_k t), \qquad (1)$$

where $\omega_k = 2\pi k/n \ (^{rad}/_{s})$, $k = 0, \cdots, \left[\frac{n}{2}\right]$, are the Fourier frequencies, and

$$a_k = \begin{cases} \frac{1}{n}\sum_{t=1}^{n} z_t \cos\omega_k t\,, & k = 0 \text{ and } k = \frac{n}{2} \quad \text{if n is even} \\ \frac{2}{n}\sum_{t=1}^{n} z_t \cos\omega_k t\,, & k = 1,2,\dots,\left[\frac{n-1}{2}\right], \end{cases}$$

with

$$b_k = \frac{2}{n}\sum_{t=1}^{n} z_t \sin\omega_k t, \qquad k = 1,2,\dots,\left[\frac{n-1}{2}\right],$$

are Fourier coefficients. The quantity $I(\omega_k)$ defined by

$$I(\omega_k) = \sum_{t=1}^{n} z_t^2 = \begin{cases} na_0^2, & k = 0, \\ \frac{n}{2}(a_k^2 + b_k^2), & k = 1, \dots, \lceil (n-1)/2 \rceil, \\ na_{\frac{n}{2}}^2, & k = \frac{n}{2} \text{ when n is even}, \end{cases} \qquad (2)$$

which is called the periodogram [11]. The periodogram values can be interpreted in terms of variance (sums of squares) of the signals at a respective frequency or period, which provides an estimation of spectrum function. In statistical signal processing, the

periodogram is a powerful technique to detect the hidden periodicities in time series.

2.2 The cross-covariance function

The cross-covariance function is a useful measurement of the strength and direction of correlation between two time series. Given two stochastic processes x_t and y_t for $t = o, \pm1, \pm2, \ldots$, we found that x_t and y_t were jointly stationary if x_t and y_t were both univariate stationary processes while the cross-covariance function between x_t and y_t were a function of the time difference k only. In such cases, we have the following cross-covariance function between x_t and y_t [11]:

$$\gamma_{x,y}(k) = E\left[(x_t - \mu_x)(y_{t+k} - \mu_y)\right], \qquad (3)$$

for $k = 0, \pm1, \pm2, \ldots$, where $\mu_x = E(x_t)$ and $\mu_y = E(y_t)$ are means of x_t and y_t. The Fourier transform of Eq. (4) is defined as

$$f_{xy}(\omega) = \frac{1}{2\pi}\sum_{k=-\infty}^{\infty} \gamma_{xy}(k)e^{-i\omega k}, \quad 0 < \omega < \pi, \qquad (4)$$

which is called the cross-spectral density between x_t and y_t. Specifically, $f_{xx}(\omega) = f_x(\omega)$ and $f_{yy}(\omega) = f_y(\omega)$ are spectrums for x_t and y_t, respectively. Since $f_{xy}(\omega)$ is a complex function, it can be written as

$$f_{xy}(\omega) = c_{xy}(\omega) - iq_{xy}(\omega), \qquad (5)$$

where $c_{xy}(\omega)$ and $q_{xy}(\omega)$ are the real and imaginary parts of $f_{xy}(\omega)$. We can express $f_{xy}(\omega)$ in the polar function

$$f_{xy}(\omega) = A_{xy}(\omega)\exp\left(i\varphi_{xy}(\omega)\right), \qquad (6)$$

where $A_{xy}(\omega) = \left|f_{xy}(\omega)\right| = [c_{xy}^2(\omega) + q_{xy}^2(\omega)]^{\frac{1}{2}}$ is the cross-amplitude spectrum and $\emptyset_{xy}(\omega) = tan^{-1}\left[\frac{-q_{xy}(\omega)}{c_{xy}(\omega)}\right]$ is a phase spectrum. The phase spectrum diagram represents the phase shift value between x_t and y_t at each frequency. The ω-frequency components of x_t have a time delay with respect to the ω-frequency components of y_t if phase shift $\emptyset_{xy}(\omega)$ is negative. The ω-frequency components of x_t have a time advance with respect to the ω-frequency components of y_t if the phase shift $\emptyset_{xy}(\omega)$ is positive. For a given $\emptyset_{xy}(\omega)$, the shift in time units is $\frac{\emptyset_{xy}(\omega)}{\omega}$. Hence, the actual time delay between x_t and y_t at the frequency ω is equal to [11]:

$$\tau_d = -\frac{\emptyset_{xy}(\omega)}{\omega}. \qquad (7)$$

Square of the correlation coefficient between the ω-frequency components of x_t and the ω-frequency components of y_t at the frequency of ω is defined as [11, 10]

$$coh_{xy}^2(\omega) = \frac{\left|f_{xy}(\omega)\right|^2}{f_x(\omega)f_y(\omega)}, \quad 0 \ll coh_{xy}^2(\omega) \ll 1, \qquad (8)$$

where $f_{xy}(\omega)$ is the cross-amplitude spectrum, while $f_x(\omega)$ and $f_y(\omega)$ are the amplitude spectrum of the x_t and y_t series, respectively.

Hence, $coh_{xy}^2(\omega)$ is the square of coherence between the ω-frequency component of x_t and the ω-frequency component of y_t. Clearly, $0 \ll coh_{xy}^2(\omega) \ll 1$. A value of $coh_{xy}^2(\omega)$ close to one implies that the ω-frequency components of the two series are highly linearly related, and a value of $coh_{xy}^2(\omega)$ near the zero implies that they are only slightly linearly related.

3 Experimental setup

IR-T1 is a small research tokamak located at the Plasma Physics Research Center. This tokamak is an air-core tokamak without a copper shell. The main parameters of IR-T1 tokamak are presented in Table 1.

Table 1: The main parameters of the IR-T1 tokamak.

Parameters	Value
Major Radius	45 Cm
Minor Radius	12.5 Cm
Toroidal Magnetic Field	<1.0 T
Plasma Current	<40 kA
Discharge Time	<35 ms
Electron Temperature	≅ 180 eV

In this research, a combination of Rogowski, cosine, and saddle sine coils are utilized to record the signals from the displacement of the plasma column. These magnetic coils were located on the circular contour around the tokamak chamber. The cosine coil consists of cosine-L and cosine-R coils. Moreover, the saddle sine coil comprised saddle-up and saddle-down coils (Figure 1). B_τ and B_n are respectively the tangential and the normal components of the magnetic field induced outside the plasma on contour ℓ. Components of B_τ and B_n were measured via the voltages supplied by the cosine and saddle coils, respectively (Figure 1c).

The Rogowski coil is a solenoidal coil whose ends are brought around together to form a torus, as illustrated in Figure 2. The plasma current (I_p) generates a poloidal magnetic field around it and induces a voltage proportional to the magnetic field in the Rogowski coil. Therefore, by integrating all the induced voltages in the Rogowski, cosine, and saddle coils, it is possible to figure out information about plasma position in IR-T1 tokamak.

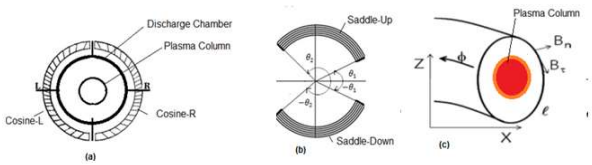

Figure 1. (a) Schematic diagram of the cosine coils, (b) Schematic diagram of the saddle sine coils, (c) Tokamak cross-section in toroidal geometry.

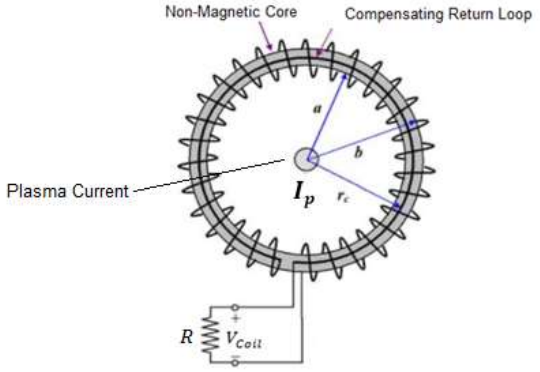

Figure. 2. Schematic diagram of the Rogowski coil in IR-T1 tokamak.

The data acquisition system (DAS) of IR-T1 is a collection of software and hardware that transform the analog signal into a digital signal. The digitalized data is stored with a time interval of 0.5μs as a time series.

4 Measurement of the time delay between signals of tokamak coils

When the plasma was in the equilibrium state, the output signals of the saddle and cosine coils were recorded as time series at a time interval of 0-35 ms. These time series were the basis of our calculations in this research. The cross-spectral analysis of the signals was performed with software SPSS and ORIGIN.

In this section, we utilized the cross-spectral analysis to calculate the time delay between the signals of magnetic coils used for measuring the plasma horizontal displacement in IR-T1 tokamak. Primarily, the time delay between the signals of the cosine coils (cosine-L and cosine-R) was calculated. For this purpose, based on Eq. (2), the periodogram of the coil signals was plotted (Figure 3). As shown in Figures. 3a and 3b, in both periodograms of cosine-L and cosine-R coils signals, the main peaks appeared at the frequency of $\upsilon = 0.33MHz$. The appearance of the main peaks at the frequency of $\upsilon = 0.33$MHz in both periodograms suggested the presence of a high linear correlation between them. The value of this correlation was calculated via Eq. (8) and its value ($\mathrm{coh}^2(\omega)$= 0.95) was represented in Figure 3c. The diagram of the phase

spectrum shows the phase shift value between two signals at the frequency in which the two signals have the highest correlation. As shown in Fig. 3d, at the frequency of $\upsilon = 0.33MHz$, the amount of phase shift between the ω-frequency components of cosine-L and cosine-R coils signals was $\emptyset_{\text{Cosine\_}L-\text{Cosine\_}R}(\omega) = -3.01$. The negative value of the phase shift indicated that the frequency components of cosine-L coil signals had a time delay with respect to the frequency components of cosine-R coil signals. By substituting this phase shift value in Eq. (7), the time delay between the cosine-L and cosine-R signals was calculated as

$$\tau_d = -\left[\frac{\emptyset_{Cosine_L - Cosi\quad R}(\omega)}{2\pi\nu}\right]$$

$$= \frac{-(-3.01)}{2(3.14)(0.33MHz)} = 1.45\ \mu s.$$

Given that the data is stored in the DAS system with an interval of 0.5 μs, it can be said that the difference in data recording between the cosine-R and cosine-Lcoils is about 3 lags.

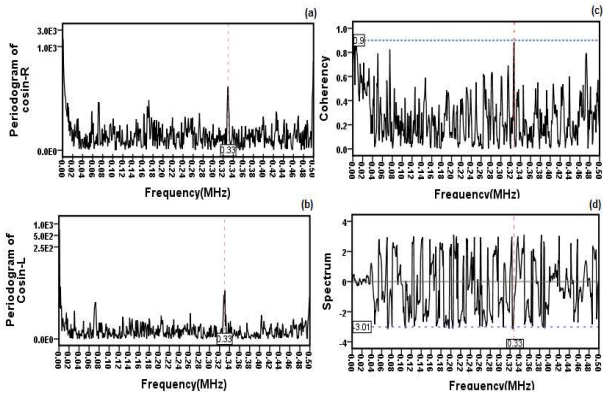

Figure 3. For $0-35$ ms (# shot No. 2017011260); (a) Periodogram of cosine-L coil signals, (b) Periodogram of cosine-R coil signals, (c) Coherence between signals of cosine-L and cosine-R coils, (d) The phase shift values between cosine-L and cosine-R coil signals.

Moreover, this method was similarly employed to measure the time delay between the saddle-up and saddle-down coils signals. As shown in Figures 4a and 4b, in both periodograms of saddle-up and saddle-down coils signals, the main peaks appeared at the frequency of $\upsilon = 0.07$MHz . The appearance of the main peaks at the frequency of $\upsilon = 0.07MHz$ in both periodograms showed the presence of a high linear correlation between them. As shown in Figs. 4c and 4d, the highest coherence ($\text{coh}^2(\omega)$= 0.98) and phase shift ($\emptyset_{Sadde-uP,\ Saddle-dow}\ (\omega) = 0.59$) between the saddle-up and saddle-down coils signals occurred at the frequency of $\upsilon = 0.07$MHz. Herein, a positive value of the average phase shift indicated that the ω-frequency components of the saddle-up signals had a time advance with respect to the ω-frequency components of the saddle-down ones. By substituting the average phase shift in Eq. (7), the time delay between the saddle-up and saddle-down coils was calculated to be $\tau_d = 1.34$ μs.

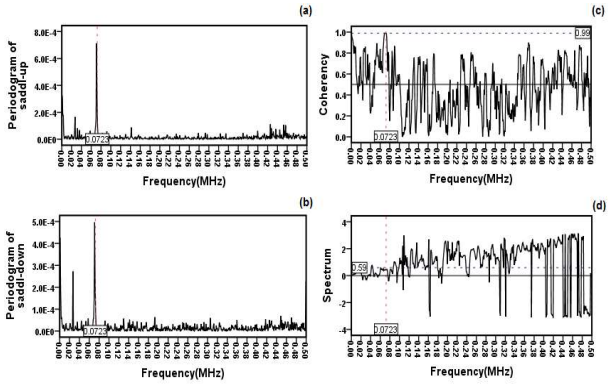

Figure 4. For $0-35$ ms (# shot No. 2017011260): **(a)** Periodogram of saddle-up coil signals, **(b)** Periodogram of saddle-down coil signals, (c) Coherence of saddle-up and saddle-down coil signals, **(d)** The phase shift values between saddle-up and saddle-down coil signals.

Also, we examined the coherence between the output data of the cosine coils without plasma. As shown in Figure 5, there is not a significant correlation at the frequency υ = 0.33 MHz as it shows that this frequency is inducted by plasma fluctuation.

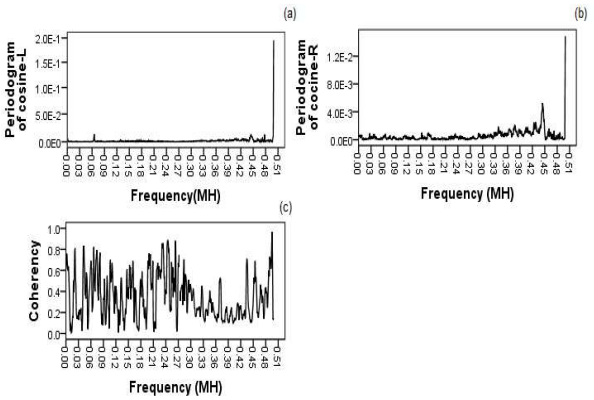

Figure 5. No plasma shot, (a) Periodogram of cosine-L coil signals, (b) Periodogram of cosine-R signals, (c) Coherence between signals of cosine-L and cosine-R coils.

5 Measurement of plasma displacement in tokamak

An m^{th} multipole moment in cylindrical coordinates $(X, \emptyset, z)$ in terms of current density is given by [12]

$$Y_m = \int J_\emptyset \, f_m ds_\emptyset = \frac{1}{\mu_0 I_p} \oint [f_m \, B_\tau + (R_0 + x) g_m B_n] \, dl, \quad (9)$$

where $J_\emptyset$ is the toroidal current density, I_p is the plasma current, while B_τ and B_n are respectively the tangential and the normal components of the magnetic field outside the plasma on contour l surrounding S_φ (see Figure 7). Features f_m and g_m are weighting factors that satisfy the following differential equations

$$\frac{\partial^2 f}{\partial^2 X} - \frac{1}{X}\frac{\partial f}{\partial X} + \frac{\partial^2 f}{\partial^2 z} = 0,$$
$$\frac{\partial g}{\partial z} = -\frac{1}{X}\frac{\partial f}{\partial X},$$
$$\frac{\partial g}{\partial X} = -\frac{1}{X}\frac{\partial f}{\partial z}, \quad (10)$$

Zakharov and Shafranov calculated the weighting factors for large aspect-ratio tokamak as [12]

$$\Delta R_{\text{Motion}} \quad f_0 = 1, \quad g_0 = 0, \quad f_1 \cong x, \quad g_1 \cong \frac{z}{R}, \quad (11)$$
$$\Delta z_{\text{Motion}} \quad f_0 = 0, \; g_0 = -1, \quad f_1 \cong z, \quad g_1 \cong \frac{x}{R}, \quad (12)$$

in which ΔR and Δz express horizontal and vertical displacements, respectively.

The first moment of Y_m describes the position of the plasma while the higher moments provide information about the plasma shape at the cylindrical coordinates. When $m = 0$, Eq. (9) yields

$$\mu_0 I = \oint B.dl, \quad (13)$$

which is the well-known Amper's Law.

The relation between two Cartesian coordinate systems, one (x,z) centered in plasma while the other that is denoted with (ξ,η) centered in contour l (see Fig. 7), are presented as

$$\xi = x + \Delta R, \quad R = R_0 + \Delta R, \quad \eta = z + \Delta z, \quad \text{and } X = x + R = \xi + R_0. \quad (14)$$

By defining the center of the plasma at the point where $(Y_{1x} = Y_{1z} = 0)$ and substituting Eqs. (11) and (14) in Eq. (9), the plasma horizontal displacement could be extracted from the first moment Y_1 as

$$\Delta R = \frac{1}{\mu_0 I_p}\left[\oint (\xi B_\tau + \eta B_n) dl + \frac{1}{R_0}\left(\frac{1}{2}\xi^2 B_\tau + \xi \eta B_n dl\right)\right]. \quad (15)$$

By considering $\xi = \rho\cos\omega t$, $\eta = \rho\sin\omega t$, and $dl = \rho d\omega$, the dependencies of fields B_τ and B_n on the polar angle ω can be Fourier transformed as [12]

$$B_\tau = \frac{\mu_0 I_p}{2\pi\rho}\left[1 + \sum_{n=1}^{n=\infty}(\lambda_n \cos n\omega + \delta_n \sin n\omega)\right], \quad (16)$$

$$B_n = \frac{\mu_0 I_p}{2\pi\rho}\sum_{n=1}^{n=\infty}(u_n \sin n\omega + k_n \cos n\omega), \quad (17)$$

where ω is the polar angle measured relative to the center of the contour l in the (η, ξ) coordinate system. The k_n and δ_n terms are needed for Δz motion and the λ_n and u_n terms are needed for ΔR motion that is investigated in this research. The integrals in Eq. (15) have been calculated in [12]. By substituting these integrals in Eq. (15), ΔR will be obtained with

$$\Delta R = \frac{r_m}{2}[\lambda_1 + \mu_1] + \frac{{r_m}^2}{4R_0}, \quad (18)$$

where r_m is the radius of the coils on the tokamak torus, λ_1 and μ_1 are

$$\lambda_1 = \frac{2r_m}{\mu_0 I_p}\int B_\tau \cos\omega d\omega,$$

and

$$\mu_1 = \frac{2r_m}{\mu_0 I_p}\int B_n \sin\omega d\omega.$$

Accordingly,

$$\Delta R = \frac{{r_m}^2}{\mu_0 I_p}\left(\int B_\tau \cos\omega d\omega + \int B_n \sin\omega d\omega\right) + \frac{{r_m}^2}{4R_0}, \quad (19)$$

where ω is the polar angle measured relative to the center of contour l in the (η, ξ) coordinate system. The components of $\int B_\tau \cos\omega d\omega$ and $\int B_n sin\omega d\omega$ were measured with voltages supplied by the cosine and saddle coils, respectively. Figure 6 depicts the circuit used for measuring the voltages supplied by the cosine and saddle coils. In this circuit, $V_s(i)$ and $i(t)$ are the coaxial cable output signal and current, respectively.

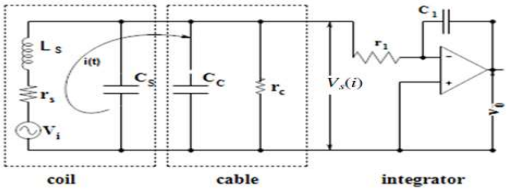

Figure 6. Block diagram of the circuit for the magnetic coils [13].

The application of Kirchhoff's voltage law for this circuit yields the following equation

$$L_s \frac{di(t)}{dt} + (r_s + r_c) = V_i(t), \quad (20)$$

Where r_s is probe resistivity, r_c the cable resistivity and L_c probe self-inductance. By Solving Eq. 20, we have [13]:

$$i(t) = \frac{1}{r_s + r_c}\left\{\frac{a_0}{2} + \sum_{n=1}^{\infty} A_n \sin(\omega_n t + \phi_n)\right\}. \quad (21)$$

Also, in the circuit (6) we have:

$$V_s(t) = r_c i(t). \quad (22)$$

Substituting Eq. (21) in Eq. (22), the coaxial cable output signal is given by

$$V_s = \frac{r_c}{r_s + r_c}\left\{\frac{a_0}{2} + \sum_{n=1}^{\infty} A_n \sin(\omega_n t + \phi_n)\right\}, \quad (23)$$

and, from Eq. (20) we have

$$V_s(t) = \frac{r_c}{r_s + r_c} V_i(t). \quad (24)$$

Also the integrator output V_0 of Figure 6 is given by

$$V_0(t) = \frac{r_c}{r_c + r_s}\frac{1}{r_1 C_1}\int V_i(t)dt = k\int V_i(t)dt, \quad (25)$$

where, r_1C_1 is the integrator time constant and $k = \frac{r_c}{r_c+r_s}\frac{1}{r_1C_1}$. Equation (24) is the input voltage to the measurement system, where V_i the inductive voltage is supplied by each of the coils, which were placed around the IR-T1 tokamak vacuum chamber. By using Faraday's law for cosine coil with variable winding $n(\omega) = n_0 cos\omega$, the induced voltage was obtained as

$$V_i(t) = n_0 r_m A k \int \frac{dB_\tau}{dt}\cos\omega d\omega. \quad (26)$$

According to Eq. (25) after integrating Eq. (26) we have

$$V_{0cosine}(t) = n_0 r_m A k \int B_\tau \cos\omega d\omega. \quad (27)$$

Here n_0 is the number of turns per length, A is the cross-section of cosine coil, r_m is the radius cosine coil. By integrating Eq. (27) for each right and left part of the cosine coil, we can write

$$\int B_\tau \cos\omega d\omega = \frac{1}{r_m n_0 k A}[V_{0R\mathrm{Cosine}}(t) - V_{0L\mathrm{Cosine}}(t)]. \quad (28)$$

The saddle coil can be designed with a variable with, $d(\omega) = d_0 \sin\omega$, but this design is complicated for construction, then we can expand $d(\omega)$ according to the Fourier expansion [14], as shown in Fig. 1b.

$$d(\omega) = \begin{cases} \Delta_0 & \theta_1 < \omega < \theta_2 \\ -\Delta_0 & -\theta_1 < \omega < \theta_2, \\ 0 & otherwise \end{cases}$$

where Δ_0 is the width of the saddle coil and

$$\theta_1 = \cos^{-1}\left(\frac{a}{R_0} - \frac{\pi}{3}\right), \theta_2 = \left(\theta_1 + \frac{2\pi}{3}\right).$$

So $d(\omega)$ can be written as

$$d(\omega) = \frac{2\Delta_0}{\pi}(\cos\theta_1 - \cos\theta_2)\sin\omega + \cdots$$

After integration from the inductive voltage of the saddle coil, we have

$$V_0(t) = N r_m d_0 k' \int B_n \sin\omega d\omega, \quad (29)$$

where N is the turn number of saddle coil and r_m is the radius saddle coil and d_0 is

$$d_0 = \frac{2\Delta_0}{\pi}(\cos\theta_1 - \cos\theta_2).$$

So, $\int B_n \sin\omega d\omega$ can be obtained by saddle coil, so that winding of saddle-up coil is vise versa the saddle-down. By integrating Eq. (29) we have

$$\int B_n \sin\omega d\omega = \frac{1}{r_m N k' A}[V_{0saddle-up}(t) - V_{0saddle-down}(t)], \quad (30)$$

where r_m is the radius of the cosine coil, n_0 is the turns per length of cosine coil, A is the cross-section of coils, N is the turns of saddle coil, while k and k' are respectively time constants of integrators as their values depend on the characteristics of the circuit (6). By substituting Eqs. (28) and (30) in Eq. (19), the plasma horizontal displacement in IR-T1 tokamak is obtained as

$$\Delta R_{multipole} = \frac{r_m}{\mu_0 I_p n_0 k A}[V_{0Cosin_R}(t) - V_{0Cosi\ _L}(t)] + \frac{r_m}{\mu_0 I_p N k' A}\left[V_{0saddle-up}(t) - V_{0saddle-down}(t)\right] + \frac{{r_m}^2}{4R_0}. \quad (31)$$

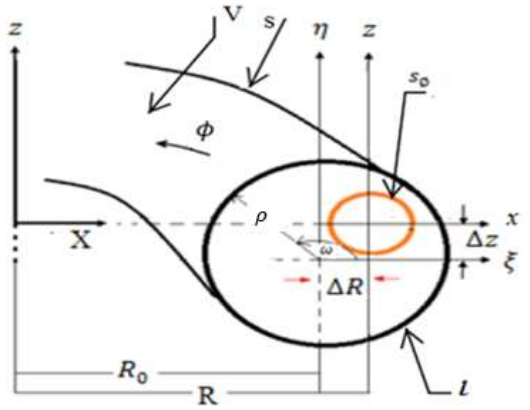

Figure7. The geometry is used for the multipole moments method

5 Results and discussion

This study was based on the signals obtained from the cosine (cosine-R and cosine-L), saddle (saddle-up and saddle-down), and Rogowski coils installed on the outer surface of the IR-T1 tokamak chamber. The temporal profile of the signals obtained from these coils was shown in Figure 8.

In Section 5, we showed that the plasma horizontal displacement was calculated via Eq. (31). The output signals of cosine and saddle coils were used in Eq. (31) for measuring the plasma horizontal displacement. In addition, in Section 4, we calculated a time delay between the signals of different parts of cosine and saddle coils; that is, $\tau_d = 1.45$ μs for cosine coils and $\tau_d = 1.34$ μs for saddle coils.

In this section, we investigate the effect of the time delay between the signals of coils on the measurement of plasma horizontal displacement. To this end, the transformations $t \to t + 1.34$ μs and $t \to t - 1.45$ μs were performed on the saddle-down and cosine-L parts of Eq. (31), respectively. By performing these transformations on Eq. (31), a new equation was obtained in which the time delay between coil signals was eliminated:

$$\Delta R_{multipole} = \frac{r_m}{\mu_0 I_p n_0 k A}[V_{0Cosin_R}(t) - V_{0Cosi\ _L}(t-1.45)] + \frac{r_m}{\mu_0 I_p N k' A}[V_{0saddle-u}\ (t) - V_{0saddle-down}(t+1.34)] + \frac{{r_m}^2}{4R_0}. \quad (32)$$

Now, we have a modified formula for measuring the horizontal displacement of plasma in IR-T1 tokamak. When the plasma is in an equilibrium state, in the time interval of 0-35 ms, we used Eq. (31) and Eq. (32) to measure the plasma horizontal displacement in IR-T1 tokamak. The results of these measurements were demonstrated in Figure 9. As shown in Fig., the red and blue lines show the horizontal displacement of the plasma which were calculated using Eq. (31) and Eq. (32), respectively. At the time interval of 0-35 ms, the comparison between the two graphs indicated a difference (2.5 mm) between the measurements of plasma horizontal displacement. Therefore, the results showed that the elimination of time delay between magnetic coil signals modified the measurement of plasma horizontal displacement in IR-T1 tokamak.

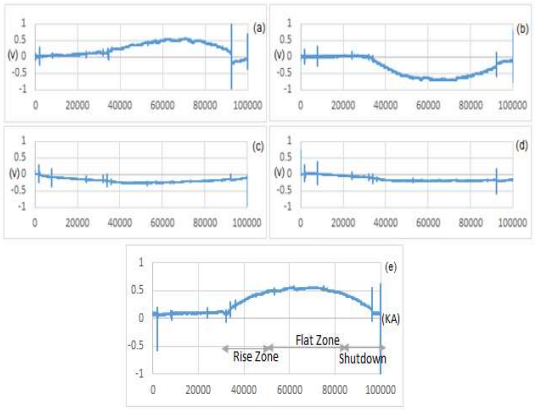

Figure 8. The time evolution of (a) cosine-R, (b) cosine-L, (c) saddle-up, (d) saddle-down coil signals, and (e) plasma current.

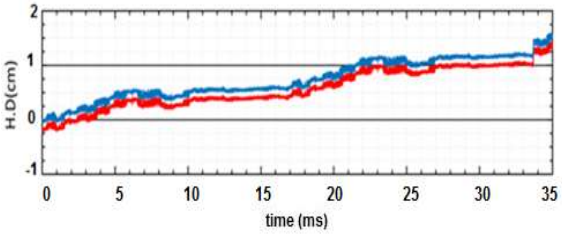

Figure 9. In the time interval of 0-35 ms (# shot No. 2017011260), the plasma horizontal displacement was measured using the multipole moment method. The red line shows the horizontal displacement of the plasma calculated using the original Eq. (22). The blue line shows the horizontal displacement of the plasma calculated using the optimized Eq. (23).

5 Conclusions

In the current paper, we presented a statistical method for measuring the time delay between the signals of magnetic coils in order to optimize the plasma displacement measurement in IR-T1 tokamak. The plasma horizontal displacement was measured using the multipole moment method.

The combination of cosine and saddle sine coils was installed on the outer surface of the IR-T1 tokamak chamber to record the signals from the plasma position. The results implied a time delay between the signals of these magnetic coils, which were $\tau_d = 1.45\mu s$ and $\tau_d = 1.34\mu s$ for cosine and saddle coils, respectively. After removing these lag times from the coil signals, a modified equation was extracted for calculating the horizontal plasma displacement in IR-T1tokamak.

The results obtained through the modified equation showed that the measurement of plasma horizontal displacement was optimized in IR-T1 tokamak. As shown in Figure 9, the value of this optimization is $\Delta R_{multipole} = 2.5\text{mm}$.

References

[1] J. Sentkerestiová, I. Ďuran, E. Dufkova, and V. Weinzettl, "Comparative measurements of plasma position using coils, hall probes, and bolometers on CASTOR tokamak" Czechoslovak Journal of Physics, **56** (2006) 138.

[2] S. V. Mirnov, "A probe method for measuring the displacement of the current channel in cylindrical and toroidal discharge vessels." Journal of Nuclear Energy, **7** (1965) 325.

[3] L. E. Zakharov and V. D. Shafranov, Equilibrium of a toroidal plasma with noncircular cross-section, (Moscow: IV Kurchatov Institute of Atomic Energy, 1973).

[4] V. S. Mukhovatov and V. D. Shafranov, "Plasma equilibrium in a tokamak." Nuclear Fusion, **11** (1971) 605.

[5] S.Santoso, E. J. Powers, D, Bengtson, and A.Ouroua, "Time-series analysis of nonstationary plasma fluctuations using wavelet transforms." Review of Scientific Instruments, **68** (1997) 898.

[6] M. Jakubowski, R. J. Fonck, C. Fenzi, G. R. McKee, " Wavelet-based time-delay estimation for time-resolved turbulent flow analysis." Review of Scientifc Instruments, **72** (2001) 996.

[7] D. Sondak, R. Arastoo, E. Schuster, and M.L Walker, "Remediation of time-delay effects in tokamak axisymmetric control loops by optimal tuning and robust predictor augmentation." Fusion Engineering and Design, **86** (2011) 1112.

[8] M. Emami, M. Ghoranneviss, and R. Tarkeshian, "Comparative study of plasma position measurements using multipole moments and discrete magnetic probes methods on IR-T1 tokamak." Fusion Engineering and Design, **83** (2008) 68488.

[9] M. Razavi, M. Mollai, P. Khorshid, I. Nedzelskiy, and M. Ghoranneviss, "Plasma column displacement measurements by modified Rogowski sine-coil and Biot–Savart/magnetic flux equation solution on IR-T1 tokamak." Review of Scientific. Instruments, **81** (2010) 053504.

[10] C. Chatfield, The Analysis of Time Series: An Introduction, (Florida: CRC Press, 2016).

[11] W. W. Wei, Time Series Analysis Univariate and Multivariate methods, (Boston: Pearson Addison Wesley, 2006).

[12] I. P. Shkarofsky, "Evaluation of multipole moments over the current density in a tokamak with magnetic probes." Physics of Fluids, **25** (1982) 89.

[13] R. Lopez-Callejas, J. S. Benıtez-Read, L. C., Longoria-Gándara, and J. Pacheco-Sotelo, "Plasma position measurement on the Novillo tokamak." Fusion Engineering and Design, **54** (2001) 21.

[14] L. Chen, Q. Zhao, Y. Zhu, Z.Fang, and H. Fan, "Measurement of plasma position on HT-7 tokamak." Fusion Engineering and Design. **34** (1997) 721.